

Agglomeration of magnetite nanoparticles with citrate shell in an aqueous magnetic fluid

Ivan V. Pleshakov^{1,a}, Vyacheslav A. Ryzhov^{2,b}, Yaroslav Yu. Marchenko^{2,c}, Arseniy A. Alekseev^{3,d}, Elina K. Karseeva^{3,e}, Vladimir N. Nevedomskiy^{1,f}, Andrey V. Prokof'ev^{1,g}

¹Ioffe Institute, St. Petersburg, Russia

²Petersburg Nuclear Physics Institute named by B. P. Konstantinov of National Research Centre “Kurchatov Institute”, Gatchina, Russia

³Peter the Great St. Petersburg Polytechnic University, St. Petersburg, Russia

^aivanple@yandex.ru, ^bvaryzhov@yandex.ru, ^c046_slava@mail.ru, ^darseniy.alekseev98@gmail.com, ^eelina.nep@gmail.com, ^fnevedom@mail.ioffe.ru, ^gAndrey.prokofyev@algo-spb.com

Corresponding author: Ivan V. Pleshakov, ivanple@yandex.ru

PACS 75.50.Mm; 75.50.Tt

ABSTRACT In this work, the aggregation of nanoparticles in an aqueous colloidal solution of magnetite, stabilized by creating a citrate shell on the particle surface is studied. Electron microscopy and laser correlation spectroscopy were used as experimental methods. Optical measurements were carried out both at zero external magnetic field and in the fields differently oriented relative to the probing laser beam. It is shown that the samples tend to form large aggregates even without the application of the field, and in the case of its presence the behavior of these structures has features that distinguish them from other magnetic fluids.

KEYWORDS magnetic fluid, aggregation, citrate stabilization, electron microscopy, laser correlation spectroscopy.

FOR CITATION Pleshakov I.V., Ryzhov V.A., Marchenko Ya.Yu., Alekseev A.A., Karseeva E.K., Nevedomskiy V.N., Prokof'ev A.V. Agglomeration of magnetite nanoparticles with citrate shell in an aqueous magnetic fluid. *Nanosystems: Phys. Chem. Math.*, 2023, **14** (3), 334–341.

1. Introduction

Magnetic fluids, or ferrofluids, are a special type of colloids with magnetic properties [1, 2]. The solid phase of these substances is a magnetically ordered material (very often, magnetite) in a nanodispersed state, and various liquid media are used as carriers, such as kerosene, water, oil, etc. As in many other colloids, when creating these systems, special techniques are used to stabilize them, that is, to prevent the adhesion of magnetic nanoparticles, for example, by coating them with a layer of surfactant. Differently stabilized ferrofluids may differ noticeably in their characteristics.

Being an interesting physical object, magnetic fluids have attracted the attention of researchers for several decades. As a result, a number of novel phenomena associated with their nanostructural nature combined with magnetism were discovered in them. In addition, it was also found quite a large number of applications. Recently, the practical proposals in this area has begun to increase rapidly, which, in turn, has given a rise to new directions, including those focused on fundamental problems.

Photonics and electronics (magnetically controlled elements [3, 4]), as well as biomedical studies considering all possible aspects of the behavior of magnetic nanoparticles embedded in the biological medium can be named as the fields developing ideas pertaining to ferrofluids [5, 6].

Physical, in particular, optical effects in ferrofluids are largely determined by the structures that nanoparticles form in them. It is well known that an external magnetic field usually leads to the appearance of extended aggregates that grow with its increase [7]. However, even without a field, objects consisting of many nanoparticles normally appear in a magnetic fluid due to coagulation. For the areas mentioned above, it is important to study the processes and features of aggregation, which provide the key to understanding the capabilities of magnetic fluids. These studies cannot be considered as complete, since fluids of different compositions and stabilized by different approaches have different properties, and currently are the subject of active investigation. This work is devoted to an aqueous solution of magnetite particles in a citrate shell, demonstrating, as will be seen from the following, significant differences from other aqueous colloids of this material.

2. Samples

Iron oxide nanoparticles were obtained by co-precipitation of iron salts ($\text{Fe}^{2+}/\text{Fe}^{3+} = 2/1$) with an excess of ammonium hydroxide according to the scheme described earlier in [8]. The reaction was carried out in an inert nitrogen atmosphere at a temperature of $80\text{ }^{\circ}\text{C}$. The resulting iron oxide Fe_3O_4 was washed with distilled water to a neutral pH, after which it was separated by a magnet. A sample of 2.3 g wet oxide was suspended in 10 ml of 1 mM aqueous solution of citric acid monohydrate at pH = 5. Then the liquid obtained was subjected to ultrasonic treatment for 60 minutes at $90\text{ }^{\circ}\text{C}$, and after that it was cooled to room temperature [9–11]. The starting point for further experiments was a sample with a solid phase concentration of 6.8 mg/ml, which was stored at $4\text{ }^{\circ}\text{C}$. In the various cases described below, it could be diluted to the desired concentrations and subjected to additional sonification.

3. Experimental techniques

3.1. Electron microscopy

Transmission electron microscopy (TEM) studies were performed at the “Material science and characterization in advanced technology” in the Ioffe Institute by JEM-2100F microscope (JEOL Ltd., Japan) at an accelerating voltage of 200 kV. Sample particles were imaged mainly under two-beam conditions in bright field mode.

Samples were prepared in the traditional way adapted to specific conditions by the following steps: 1) dilution of the initial colloidal solution by approximately 20 times with distilled water, 2) dispersion of the resulting solution with ultrasound for 8–10 min, 3) immersion in the resulting solution of a special mesh for TEM studies with a thin supporting carbon film already applied to it, on which the solution was deposited, 4) drying the obtained sample under normal conditions for 30 minutes.

3.2. Laser correlation spectroscopy

It is known that laser correlation spectroscopy is an effective tool for studying clusters in solutions containing nanoparticles; in particular, it has been successfully used to characterize ferrofluids placed in a magnetic field [12–14]. This method is based on the calculation of the autocorrelation function of the light scattered by the sample, from which, with a known viscosity of the carrier liquid, data on the sizes of particles or their agglomerates d are extracted (a more detailed description of this technique can be found in [14] and references therein).

To implement the method, we used the installation, the block diagram of which is shown in Fig. 1. The laser beam was focused by an optical system on a magnetic fluid placed in a cuvette located in the Helmholtz coils that create a magnetic field H .

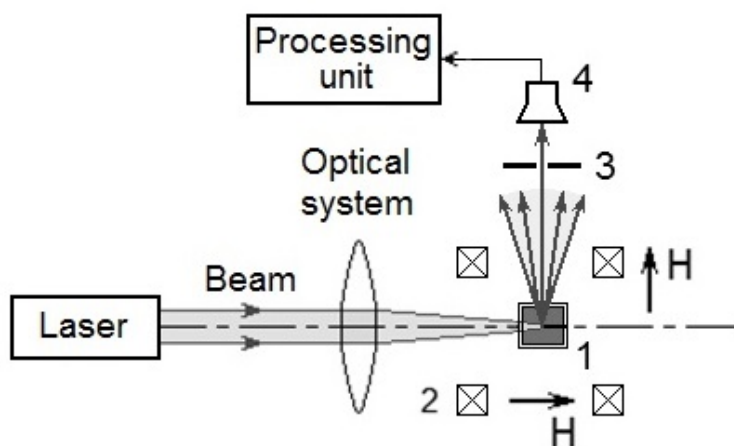


FIG. 1. Experimental setups for laser correlation spectroscopy: 1 – sample (cuvette with magnetic fluid); 2 – Helmholtz coils; 3 – diaphragm; 4 – photomultiplier. Possible orientations of the field H are shown

Scattered radiation that passed through the diaphragm at an angle of 90 ° with respect to the optical axis of the system was recorded by a photomultiplier, and then the electrical signal was digitized and processed on a computer. The results of the analysis were displayed as a normalized scattering intensity versus d . We used a special algorithm for determining the size of scatterers, described in [15], the characteristic time of one measurement procedure, dependent on the time of signal accumulation and processing, was 2–3 min. In the measurements, a He-Ne laser with a wavelength of $\lambda = 632.8\text{ nm}$, high stability and a narrow spectral line was used. Scattered light was detected in a plane perpendicular to the plane of polarization of the incident beam.

To ensure single scattering, in laser correlation spectroscopy experiments the sample was diluted to a particle concentration of 10^{-3} vol. %.

The experimental setup was similar to that used earlier in [14], but in this case, the design of the Helmholtz coils made it possible to orient the magnetic field H created by them both parallel to the optical axis of the system and perpendicular to it (in the direction of scattered light propagation). The field strength could vary within 0–400 Oe.

4. Results of experiments

The microstructure of the sample obtained by the deposition is shown in Fig. 2. By these electron micrographs, one can make an estimate of the average size of nanoparticle, which, as can be seen from Fig. 2a and Fig. 2b is about 10 nm, which does not differ from the data typical for other similar materials [16, 17]. An essential circumstance is that the pattern observed at a different scale (Fig. 2b,c,d) indicates the appearance of large formations of many nanoparticles in the deposited layer, reaching significant dimension of hundreds of nanometers. Most likely, the formation of similar aggregates still occurs in the liquid state (although such factors as surface tension, the effect of the surface on which the deposition occurs, etc. should affect their shape and size after the deposition process is completed). It should be emphasized that the images in Fig. 2 were obtained without applying an external magnetic field.

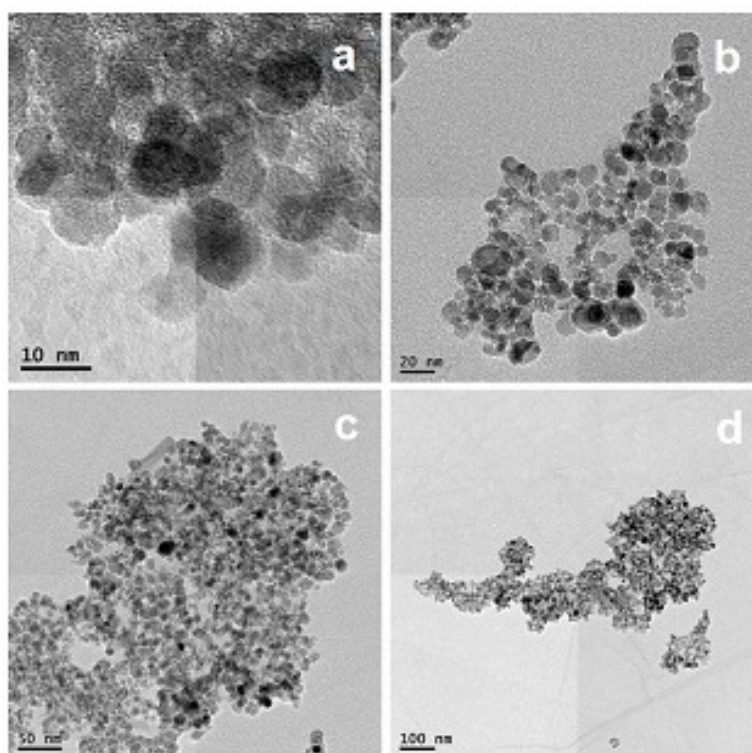


FIG. 2. Electronic micrographs of ferrofluid sediment at different scales (shown in the figure)

In experiments on laser correlation spectroscopy, it was found that the results of measurements performed after the application of the magnetic field depend on time. This reflects the evolution of forming aggregates peculiar to ferrofluids, which occurs rather slowly (with a characteristic time of the order of minutes) [14]. Keeping this in mind, the study of aggregation processes was carried out as follows: first, data were obtained at $H = 0$, then the field was switched on, and after some time, chosen in such a way that the total interval from the moment of the switching on to the end of the measurement was five minutes, the data collection procedure was started. The initial values of the average sizes of scatterers d_0 and, consequently, the distribution functions of d obtained for a nonzero field could depend on the preliminary preparation of the samples, but the qualitative behavior of the system always remained the same. (The value of d_0 is understood further as such a d at which, when $H = 0$, the local maximum in the aggregate size distribution is reached.)

Examples of distribution functions d taken at different times and for different field orientations are shown in Fig. 3 ($H = 380$ Oe). Because of the fact that in these experiments the spread of data was quite large, they were smoothed using the sliding window algorithm with the number of points in the window equal to five. In all measurements, the distribution pattern turned out to be quite complex, containing many peaks, each of which was assigned its own value d_0 .

In the case of measurements with a parallel orientation of the field (Fig. 3a), the solution was subjected to ultrasonic treatment and settled for two days before measurements were taken, and with a perpendicular orientation (Fig. 3b), the difference was that the measurements were carried out after two weeks. As can be seen, the numerical values of d differed

here; in general, we found that the values of d_0 , i.e., those from which every particular measurement began, could vary substantially depending on the prehistory of the sample. Nevertheless, qualitatively the behavior of the system, as well as the data obtained for relative values, was reproduced quite well from experiment to experiment.

From graphs like those shown in Fig. 3, several peaks were distinguished, that assuredly observed in most experiments (it should be noted that at certain points in time some peaks disappeared, and new ones could also appear). Each was described satisfactorily by log-normal distribution:

$$f(d) = \frac{A}{\sqrt{2\pi}\sigma d} \exp\left[-\frac{(\ln \frac{d}{d_0})^2}{2\sigma^2}\right], \quad (1)$$

where A and σ are parameters (along with d_0 used in the fitting). Statistical characteristics of the distributions indicated in Fig. 3 as 1 and 2 are summarized in Tables 1 and 2, which refer to the parallel and perpendicular field orientations, respectively (additional rows reflect the appearance of additional peaks). Here d_0 is the median, $\mu = \ln d_0$.

The time behavior of the relative average size of aggregates d/d_0 belonging to groups 1 and 2 is shown in Fig. 4 (the first and the last points on this graph correspond to $H = 0$). The field had no effect on fine structural elements (at $d \sim 40$ – 60 nm).

The dependence of the sizes of large aggregates on H under the conditions of their temporal evolution can be obtained only with a certain degree of conventionality, since along with their growth during the measurement, the opposite process must occur as can be seen from Fig. 4. However, a rough idea of it may be the result of the experiment, which is set as follows: after each increase in the field, a measurement is performed (which, as mentioned above, takes 2–3 min), and then the field is immediately increased and the procedure repeated. The outcome taken in this way for a perpendicular orientation of the magnetic field is shown in Fig. 5.

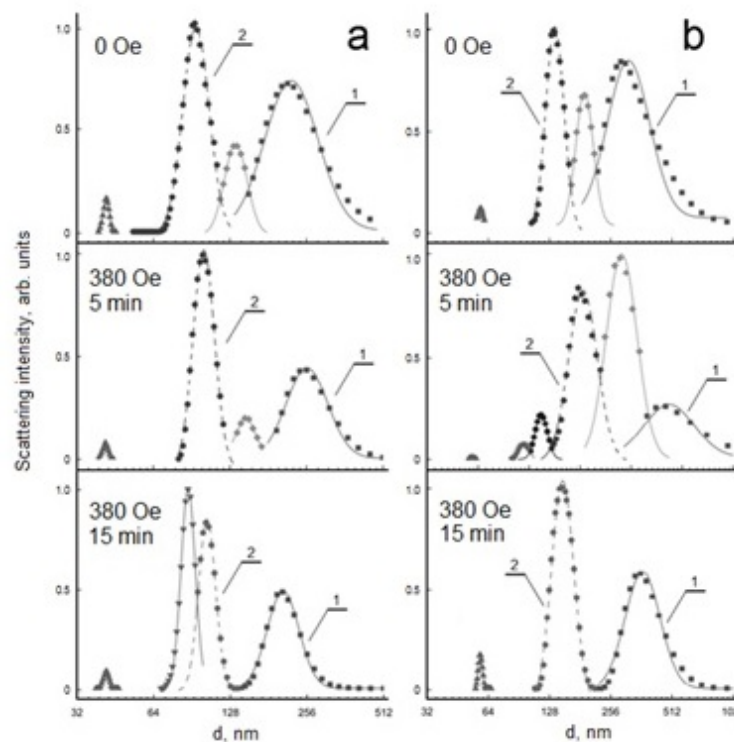


FIG. 3. Examples of size distributions of agglomerates for the cases of: a) parallel orientation of the magnetic field H with the optical axis and b) perpendicular orientation of the magnetic field H with the optical axis ($H = 380$ Oe). 1, 2 – selected groups of agglomerates, for which the dependences of their relative parameters are given further

5. Discussion

The obvious conclusion that follows from the above experimental results is that in the initial state, the nanoparticles of the ferrocolloid under study are mainly belong to large formations, for which the applied magnetic field, at first, has the expected effect, i.e. leads to their growth. Further, the particle size distribution (Fig. 3) begins to evolve, demonstrating, despite the presence of the field, a gradual decrease in the size of these aggregates in the time interval of 5–15 min (Fig. 4). We can approximately assume that at the time of H switching off ($t = 20$ min), the system returns to its original position.

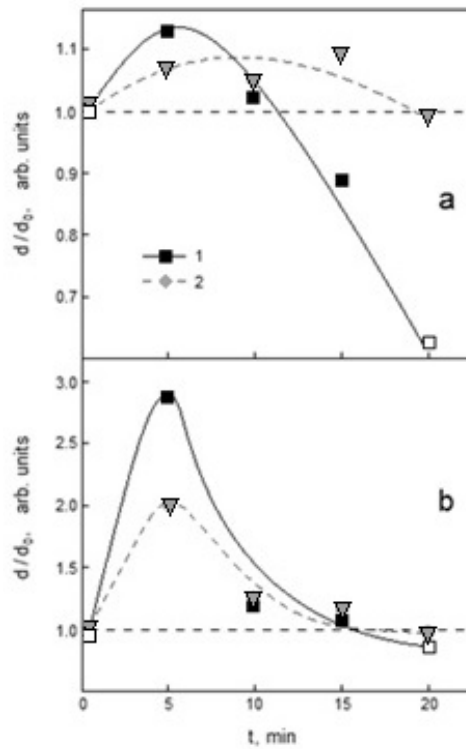


FIG. 4. Time dependences of the relative sizes of agglomerates for a) parallel geometry of experiment and b) perpendicular geometry of experiment ($H = 380$ Oe). 1 – group 1, 2 – group 2 (open symbols correspond to $H = 0$)

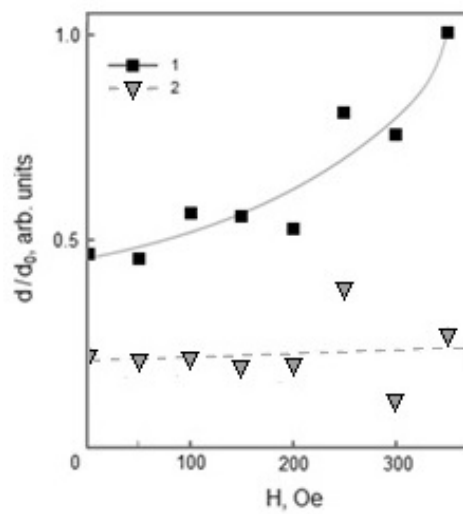


FIG. 5. Field dependences of the relative medium sizes of agglomerates (groups 1 and 2) for perpendicular geometry of experiment (normalized on the medium size d_0 in group 1 at the maximum value of the field).

TABLE 1. Parallel geometry of the experiment

H , Oe	Time of action t , min	d_0 , nm
0	0	237.02
		136.49
		95.49
		41.81
380	5	266.93
		148.83
		102.08
		41.49
380	10	242.06
		99.86
		76.59
		41.36
380	15	210.62
		104.38
		87.82
		41.72
0	20	148.41
		94.56
		73.97
		41.66

The effect of differently orientated fields are markedly distinguished: as can be seen from the comparison of Fig. 4a and Fig. 4b, in perpendicular geometry, at the initial stage a much more significant change in the relative value d/d_0 is recorded. Since the laser correlation spectroscopy is sensitive to the size of scatterers in a plane orthogonal to the optical axis, the registration of this phenomenon reflects the formation of structures elongated parallel to H , which is always observed in such materials. From Fig. 4, it is easy to determine that at $H = 380$ Oe, the longitudinal size of the aggregate increases by 2–3 times, while for the transverse size the enhancement does not exceed 15 %, i.e. an increase in its volume can be estimated as half the order.

The nontrivial fact of a decrease in the value of d/d_0 at the next stage of evolution has not yet found a strict explanation, but most likely it is owing to the dynamics of large objects with many nanoparticles that do not maintain stability even at $H \neq 0$. After reaching the maximum size, aggregates decrease, and the longitudinal size decreases most rapidly. There is no ideal restoration of the initial state (some peaks of the distribution of d are shifted to the region of even slightly smaller values than at $t = 0$).

On the whole, however, it can be stated that the system tends to a certain equilibrium state, in which its structural elements have approximately the same dimensions as those formed in the colloid before external influence. Note that the spread of d values associated with each group of aggregates described by individual functions (1) is comparable with the distance between the peaks, so it is difficult to accurately determine the temporal and field behavior of the aggregates. Thus, the graphs in Fig. 4 and 5 represent only the general nature of those. However, the field dependence (Fig. 5), taken according to the method described above, still reflects the tendency for aggregates to enlarge after the switching on or increase of H , despite the opposing processes of growth and decay of these formations.

Figure 5 does not show data related to very small scatterers ($d \sim 60$ nm), since their sizes are almost independent of the field (Table 2). Perhaps this is due to the fact that they are non-magnetic inclusions that may be presented in samples because of certain peculiarities of their manufacturing.

The specificity associated with the stabilizing method of the magnetic fluid is determined by the peculiarities of the interaction of nanoparticles with a given type of surfactant deposited on their surface, that is, ultimately, from what

TABLE 2. Perpendicular geometry of the experiment

H , Oe	Time of action t , min	d_0 , nm
0	0	331.52
		192.29
		137.48
		58.63
380	5	963.26
		470.61
		276.51
		152.23
		119.72
		59.24
380	10	411.46
		171.12
		58.57
380	15	382.01
		150.89
		58.55
0	20	288.71
		131.89
		59.60

structure begins the formation of a new one after the application of the field. Idealized approach to the analysis of ferrocolloids usually considers a medium with single nanoparticles dispersed in it, which gather into clusters when a magnetic field is applied [17]. This is a simplification, since, as already was mentioned, even at $H = 0$ some amount of large particle associates are almost always presented in such substances [14]. In our case at the initial state practically all particles are already combined into very large aggregates (Fig. 2,3), which, most probably, is determined by the properties of the citrate shell. Further growth of aggregates in the field can continue up to a certain limit and then their fragmentation occurs. (It should be noted that the observed effect of the decrease of the amount of large objects cannot be explained by their sedimentation, since the characteristic time of such a process, estimated by the Stokes formula, significantly exceeds the measurement time.)

Electron microscopy confirms our assumption that nanoparticles in the studied materials tend to assemble into large formations even in the absence of the external action. Despite the fact that these data were obtained under conditions different from those under which the laser correlation spectroscopy experiments were performed, as well as the above-mentioned distortions that occur when a ferrocolloid is deposited on a substrate, the result presented in Fig. 2 provides a fairly convincing illustration of this property of our samples at a qualitative level. In the presence of agglomerates in the liquid state with dimensions of the order of hundreds of nanometers similar to those shown in the figure, after applying a magnetic field to the system, processes associated with their initial growth and subsequent fragmentation will develop.

6. Conclusion

In this paper, it is shown that large-sized aggregates can form in citrate stabilized aqueous magnetite-containing ferrofluid without external magnetic field. Besides, the presence of large formations determines the unusual behavior of the system in the field, which combines their conventional field-induced grows with the decay process. The latter begins at a certain stage, after some limiting volume of aggregate has been reached. This information should be useful in the analysis of colloids with a magnetically ordered substance dispersed in a medium of complex composition.

References

- [1] Socoliuc V., Avdeev M., Kuncser V., Turcu R., Tombácz E., Vekas L. Ferrofluids and bio-ferrofluids: looking back and stepping forward. *Nanoscale*, 2022, **14**, P. 4786–4886.
- [2] Oehlsen O., Cervantes-Ramírez S.I., Cervantes-Avilés P., Medina-Velo I.A. Approaches on ferrofluid synthesis and applications: current status and future perspectives. *ACS Omega*, 2022, **7**, P. 3134–3150.
- [3] Taghizadeh M., Bozorgzadeh F., Ghorbani M. Designing magnetic field sensor based on tapered photonic crystal fibre assisted by a ferrofluid. *Scientific Reports*, 2021, **11**(1), P. 14325.
- [4] Yong Zhao, Yuyan Zhang, R.-Q. Lv, Qi Wang. Novel optical devices based on the tunable refractive index of magnetic fluid and their characteristics. *J. Magn. Magn. Mat.*, 2011, **323**(23), P. 2987–2996.
- [5] Imran M., Alam M.M., Khan A. Advanced biomedical applications of iron oxide nanostructures based ferrofluids. *Nanotechnology*, 2021, **32**(42), P. 422001.
- [6] Pilati V., Gomide G., Cabreira Gomes R., Goya G.F., Depeyrot J. Colloidal stability and concentration effects on nanoparticle heat delivery for magnetic fluid hyperthermia. *Langmuir*, 2021, **37**(3), P. 1129–1140.
- [7] Ivanov A.O., Zubarev A.Yu. Chain formation and phase separation in ferrofluids: the influence on viscous properties. *Materials*, 2020, **13**(18), P. 3956.
- [8] Shevtsov M.A., Nikolaev B.P., Yakovleva L.Y., Marchenko Y.Y., Dobrodumov A.V., Mikhrina A.L., Martynova M.G., Bystrova O.A., Yakovenko I.V., Ischenko A.M. Superparamagnetic iron oxide nanoparticles conjugated with epidermal growth factor (SPION-EGF) for targeting brain tumors. *Int. J. Nanomed.*, 2014, **9**, P. 273.
- [9] Kotsmar C., Ki Youl Yoon, Haiyang Yu, Seung Yup Ryoo, Joseph Barth, Shao S., Prodanović M., Milner T.E., Bryant S.L., Chun Huh, Johnston K.P. Stable citrate-coated iron oxide superparamagnetic nanoclusters at high salinity. *Ind. Eng. Chem. Res.*, 2010, **49**, P. 12435–12443.
- [10] Yusuf M.S., Rahmasari S., Rahmasari R. Synthesis processing condition optimization of citrate stabilized superparamagnetic iron oxide nanoparticles using direct co-precipitation method. *Biomed. Pharmacol. J.*, 2021, **14**(3), P. 1533–1542.
- [11] Arefi M., Kazemi Miraki M., Mostafalu R., Satari M., Heydari A. Citric acid stabilized on the surface of magnetic nanoparticles as an efficient and recyclable catalyst for transamidation of carboxamides, phthalimide, urea and thiourea with amines under neat conditions. *J. Iran. Chem. Soc.*, 2019, **16**, P. 393–400.
- [12] Broillet S., Szlag D., Bouwens A., Maurizi L., Hofmann H., Lasser T., Leutenegger M. Visible light optical coherence correlation spectroscopy. *Opt. Express*, 2014, **22**(18), P. 21944–21957.
- [13] Nepomnyashchaya E., Velichko E., Aksenov E., Bogomaz T. Optoelectronic method for analysis of biomolecular interaction dynamics. *J. Phys. Conf. Ser.*, 2014, **541**(9), P. 01203.
- [14] Nepomnyashchaya E.K., Prokofiev A.V., Velichko E.N., Pleshakov I.V., Kuzmin Yu.I. Investigation of magneto-optical properties of ferrofluids by laser light scattering techniques. *J. Magn. Magn. Mat.*, 2017, **431**, P. 24–26.
- [15] Nepomniashchaia E.K., Velichko E.N., Aksenov E.T. Solution of the laser correlation spectroscopy inverse problem by the regularization method. *Univ. Res. J.*, 2015, **15**, P. 13–21.
- [16] Scherer C., Figueiredo Neto A.M. Ferrofluids: Properties and Applications. *Braz. J. Phys.*, 2005, **35**(3A), P. 718–727.
- [17] Chikazumi S., Taketomi S., Ukita M., Mizukami M., Miyajima H., Setogawa M., Kurihara Y. Physics of magnetic fluids. *J. Magn. Magn. Mat.*, 1987, **65**, P. 245–251.

Submitted 28 May 2023; accepted 5 June 2023

Information about the authors:

Ivan V. Pleshakov – Ioffe Institute, 26 Politechnicheskaya str., St. Petersburg, 194021, Russia; ORCID 0000-0002-6707-6216; ivanple@yandex.ru

Vyacheslav A. Ryzhov – Petersburg Nuclear Physics Institute named by B. P. Konstantinov of National Research Centre “Kurchatov Institute”, Gatchina, 188300, Russia; ORCID 0000-0002-0546-1805; varyzhov@yandex.ru

Yaroslav Yu. Marchenko – Petersburg Nuclear Physics Institute named by B. P. Konstantinov of National Research Centre “Kurchatov Institute”, Gatchina, 188300, Russia; ORCID 0000-0002-7923-2175; 046.slava@mail.ru

Arseniy A. Alekseev – Peter the Great St. Petersburg Polytechnic University, 29 Polytechnicheskaya str., St. Petersburg, 195251, Russia; ORCID: 0009-0000-5368-6788; arseniy.alekseev98@gmail.com

Elina K. Karseeva – Peter the Great St. Petersburg Polytechnic University, 29 Polytechnicheskaya str., St. Petersburg, 195251, Russia; ORCID 0000-0002-4416-9380; elina.nep@gmail.com

Vladimir N. Nevedomskiy – Ioffe Institute, 26 Politechnicheskaya str., St. Petersburg, 194021, Russia; ORCID 0000-0002-7661-9155; nevedom@mail.ioffe.ru

Andrey V. Prokof'ev – Ioffe Institute, 26 Politechnicheskaya str., St. Petersburg, 194021, Russia; ORCID 0009-0009-7894-1947; andrey.prokofyev@algo-spb.com

Conflict of interest: the authors declare no conflict of interest.